Wang, Haihang; Abu-Dakka, Fares; Nguyen Le, Tran; Kyrki, Ville; Xu, He

A Novel Soft Robotic Hand Design With Human-Inspired Soft Palm

Published in:
IEEE Robotics and Automation Magazine

DOI:
10.1109/MRA.2021.3065870

Published: 01/06/2021

Document Version
Publisher's PDF, also known as Version of record

A Novel Soft Robotic Hand Design With Human-Inspired Soft Palm

Achieving a Great Diversity of Grasps

By Haihang Wang, Fares J. Abu-Dakka, Tran Nguyen Le, Ville Kyrki, and He Xu

Soft robotic hands and grippers are increasingly attracting attention as robotic end effectors. Compared with their rigid counterparts, they are safer for human–robot and environment–robot interactions, easier to control, and more compliant, and they cost and weigh less. Design studies of soft robotic hands have focused mostly on the soft fingers and bending actuators. However, the palm is also an essential part in grasping. In this work, we propose a novel design for an inexpensive soft humanoid hand with pneumatic soft fingers and a soft palm. The configuration of the soft palm is based on a modular design that can be applied to actuate different kinds of existing soft fingers. The splaying of the fingers, bending of the whole palm, and abduction and adduction of the thumb are implemented by the palm. Moreover, we present a new design of soft finger, called the hybrid-bending soft finger (HBSF), that can both bend in the grasping axis and deflect in the side-to-side axis, achieving human-like motion (Figure 1). The functions of the HBSF and soft palm are evaluated both in simulation, using the Simulation Open Framework Architecture (SOFA) framework, and experimentally. Six finger designs with 1–11 longitudinal segments are analyzed. The versatility of the soft hand is evaluated and demonstrated experimentally by its grasping of objects according to Feix's taxonomy. The results demonstrate a great diversity of grasps, with 31 of the 33 grasp types of the taxonomy performed successfully with the proposed design, showing promise for grasping a large variety of objects with different shapes and weights.

Overview and Motivation

Hands and grippers are essential components in robotic manipulation as they serve as the physical interface between the robot and the objects to be manipulated. Dexterous grasping is a prerequisite for task-dependent manipulation, which requires the consideration of factors

Digital Object Identifier 10.1109/MRA.2021.3065870
Date of current version: 14 April 2021

such as interaction forces, stiffness and compliance, dexterity, and the number of degrees of freedom (DoF) [1].

Conventional rigid robotic hands for industrial applications are generally able to provide high positional accuracy, thanks to their sophisticated actuation and sensing mechanisms. However, it is hard to control the contact force between the hand and objects, as the rigid hand structure driven by electrical motors commonly generates large contact forces. In complex real scenarios, robots may often need to manipulate objects with varying shapes, sizes, and poses in uncertain environments [2]. Moreover, when the targeted objects are fragile or delicate, large contact forces can deform or damage them. Further drawbacks of these rigid hands lie in their heavy weight and high cost. Thus, soft robotic hands with passive compliance have attracted attention as inherently safe and adaptive alternatives. Not only can soft robotic hands easily adapt to objects of various shapes and sizes, but they can also achieve contact smoothly, without the need of sophisticated control as required by rigid hands. Furthermore, their soft nature helps to minimize the damage to the manipulated objects.

Figure 1. The new soft humanoid hand and the grasped objects used in this work.

Soft bending actuators, used as fingers, are the main component of soft robotic hands and grippers. These actuators can be sorted into various types, such as fluidic elastomer actuators (FEAs), cable-driven actuators, shape memory alloys, and electromagnetic/magnetic actuators. Among these, FEAs have played a particularly remarkable role in pushing the development of compliant hands. FEAs are mainly made of silicone rubber and driven by pneumatics or hydraulics. The pneumatic types of FEAs are known as soft pneumatic actuators (SPAs). The most popular SPAs are the pneumatic networks (pneu-nets), which are a class of bending actuators described in [3], and the fiber-reinforced actuators, described in [4]. Pneu-nets are bonded by two layers: a silicone-based top layer containing a network of numerous connected chambers and an inextensible bottom layer. When the actuator is inflated, the top layer extends, and the actuator achieves a bending motion. The fiber-reinforced actuator comprises an extensible chamber, an inextensible layer, and fibers. Its bending mechanism is similar to that of the pneu-nets actuator. The fiber reinforcement is used to limit the chamber in axial extension instead of useless radial expansion. Both types of actuators are simple in design, effective, and easy to fabricate.

In the literature, there are different designs and applications for soft robotic hands based on pneu-nets bending-actuator [5]–[8] and fiber-reinforced actuator prototypes [1], [9]–[12]. However, compared with each other, the pneu-nets actuator has a lower capacity of input pressure because of its total soft top layer under the same wall thickness, which limits its maximal grasping force. In addition, the fiber-reinforced one has a lower bending efficiency, which limits its bending angle under the same pressure. To overcome their shortcomings, in this article, we discuss the design of a novel HBSF in which we integrate the inner-chamber network structure inspired by pneu-nets with the fiber-reinforcement method.

Recently, there have been rapid developments in soft robotic hands and grippers. However, these improvements have focused mostly on the study of soft fingers and overlooked the importance of the palm, with the fingers usually being assembled together and fixed to a rigid palm or base. However, the palm plays a considerable role in grasping functionality, and the fixed finger position greatly limits the variety of grasp types and poses of the hands.

The ability to perform dexterous manipulation depends on the postural variability of a hand: the higher this variability, the more dexterous the hand (examples of grasping postures as in the Feix taxonomy are given in the article by Feix et al. [13]). A robotic hand with a changeable palm can adjust the position and orientation of its fingers, which can significantly improve the postural flexibility of the hand in terms of the sizes and shapes of objects that can be grasped. Sun et al. [7] presented a

flexible robotic gripper with a rigid, changeable palm. The configuration of the gripper can be adjusted using a slider and beam mechanism. An opposable thumb is important and useful for achieving dexterity in a robotic hand. However, the rigid, changeable palm can change only the position of the fingers.

The Robotics and Biology Laboratory Hand 2, designed by Deimel and Brock [1], has a soft palmar actuator for enabling thumb abduction. It has a new actuator, called *PneuFlex*, with fiber reinforcement of the soft fingers. In addition, the researchers used two connected PneuFlex actuators to form the base of the thumb to achieve better thumb dexterity. The other four fingers were fixed on a 3D-printed scaffold. The assembly angle between the thumb and the other four fingers is about 120°, instead of their being coplanar. The soft biomimetic prosthetic hand developed in [10] presents a similar design for thumb abduction. It has PneuFlex actuators as in [1] but with one applied for the thumb and two for the palm. The exoskeleton for fixing the soft actuators is deformable and based on a 3D scan of a real human hand. Both hands have soft actuators for thumb abduction. However, the palm motion for the other four fingers was ignored. The four fingers of these hands can bend in only a certain fixed direction. In contrast to the work of [1] and [10], to augment the human-like palmar function of the soft hand, we present a pneumatic soft humanoid palm that can help thumb abduction, splaying of the four other fingers, and palmar bending.

The palm plays a considerable role in grasping functionality, and the fixed finger position greatly limits the variety of grasp types and poses of the hands.

In this article, we propose a compact hybrid solution for a soft humanoid hand, as shown in Figure 1. For the sake of clarity, the main contributions of this article are

- a novel design for an HBSF, integrating an inner-chamber network structure with the fiber-reinforcement method
- a novel design for a pneumatic soft humanoid palm.

The soft robotic hand is made of soft materials only. The HBSF can robustly grasp a variety of objects with different weights, sizes, shapes, and stiffnesses. The soft humanoid hand consists of five soft pneumatic fingers and

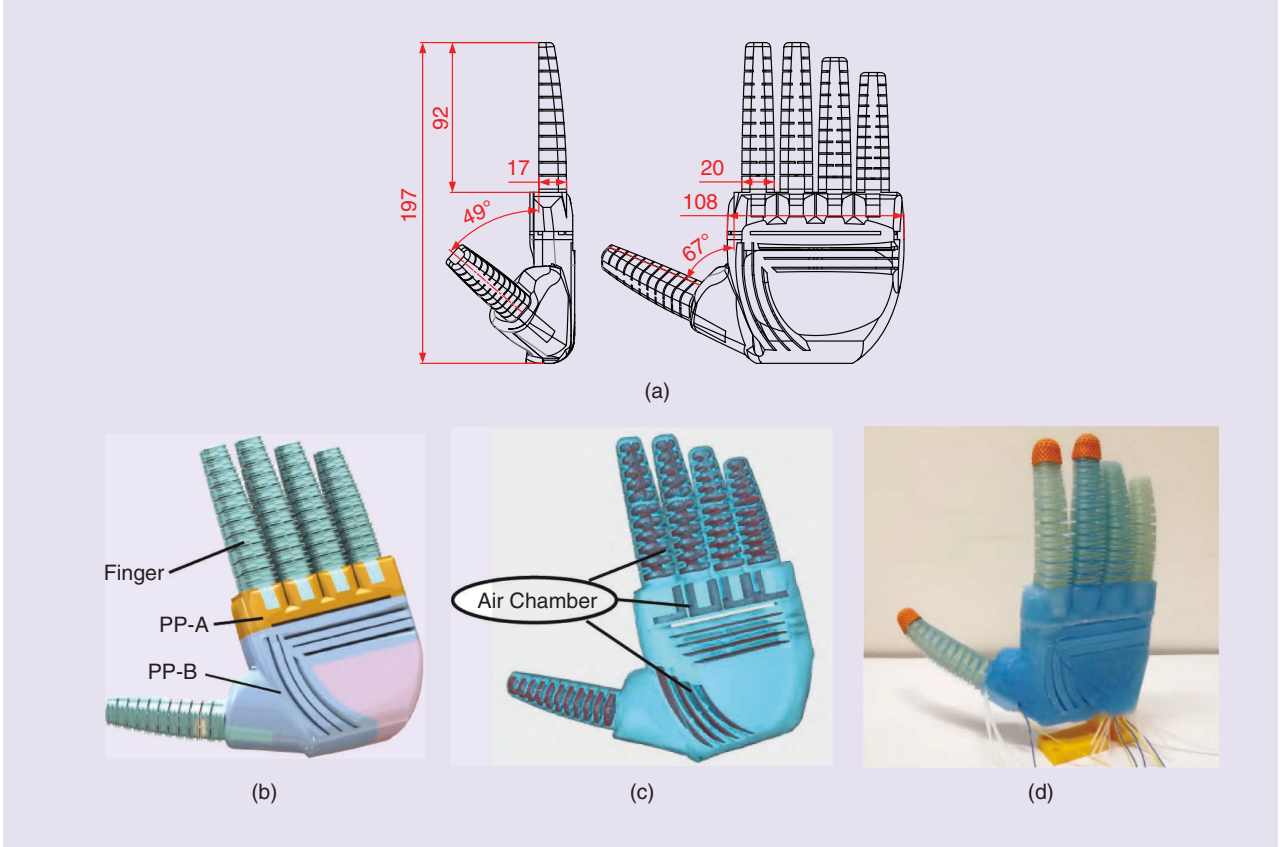

Figure 2. The proposed pneumatic soft humanoid hand with dexterous palm. (a) The hand dimensions in millimeters. (b) Its 3D model. (c) The air chambers; the red parts show the inner distribution of the air chambers, which will be pressurized based on the SoftRobots plug-in. (d) The soft robotic hand prototype.

two soft palmar parts, all of which are independent and assembled together using silicone connections.

Design and Simulation

Soft Hand

Existing designs for soft hands/grippers can be divided into two main morphological types: anthropomorphic hands and grippers with several spatially evenly distributed fingers. Here we chose an anthropomorphic design with a new dexterous soft robotic palm. Figure 2(d) presents the prototype of the soft humanoid hand, which has a weight of only 300 g. Its exact overall dimensions are presented in Figure 2(a); they are similar to those of a typical human hand. The hand is low in cost (about €100–150 for the main soft body, including silicone and tubing).

The bending motion is the basic and main function for grasping.

For this article, the soft hand [see Figure 2(b)] has three functional components: fingers, palm part A (PP-A), and palm part B (PP-B), and all are actuated pneumatically. The fingers are designed to grasp, grip, and manipulate objects through bending in the grasping axis and deflecting in the transverse axis. The five fingers are sorted as the thumb and four distal fingers (index, middle, ring, and little fingers). PP-A is used to splay the four distal fingers, which extends the distance between fingers and enlarges the grasping scope. PP-B achieves two functions: palm bending and thumb abduction and adduction.

A simulation is conducted to guide our design and ensure that the proposed design can work as intended in the actual hand. Finite-element modeling (FEM) is used to simulate and analyze the whole soft hand, as indicated in [15]. The simulation in real time is implemented in the Simulation Open Framework Architecture (SOFA) framework [14] with the SoftRobots plug-in [16]. The SOFA framework presents a fast, real-time simulation of the whole soft hand, while the soft actuators can also be more accurately simulated using high-resolution volumetric FEM analysis, such as Abaqus [9] or VegaFEM [17]. However, simulation using Abaqus requires a long computational time to obtain convergence, while VegaFEM does not implement collision detection or contact handling, hence limiting its applicability to contact scenarios. To achieve a satisfactory tradeoff between the computational load and accuracy, we choose to use SOFA. The mesh file of the soft hand consists of 40,316 tetrahedra and 11,894 nodes. The inflatable air chambers are presented in the SOFA environment, as shown in Figure 2(c).

Soft Finger

Function

In this work, we aim to develop a humanoid pneumatic soft hand with dexterous soft fingers. Among the five fingers, the functions of the thumb, index, and middle fingers are the main ones for grasp manipulation, while the ring and little fingers usually play an assistive role. The index and middle fingers in this work have two functional goals: bending in the primary grasping axis (toward the soft palm) and deflecting from side to side (perpendicular to the primary grasping direction). The function of the ring and little fingers is limited to bending motion in this work.

The bending motion is the basic and main function for grasping. The bending angles are set to about 180° to resemble those of human fingers. Side-to-side deflection motion is also useful and necessary to perform splaying and gripping between two adjacent distal fingers and rotatory movement of the object while being grasped by three fingers.

Design

The soft hand fingers, which are able to both bend and deflect, are HBSFs, based on a modular approach. HBSFs are used for the thumb, index, and middle fingers. The structures of these three fingers are identical in shape, with a length L of 90 mm, although the thumb is 20 mm shorter than the index and middle fingers. The structure of the ring and little fingers is a simplified version of an HBSF that can only flex. In the ring and little fingers, the two side-by-side chambers in one segment of the HBSF were replaced with one chamber.

In this work, the HBSF combines the advantages of pneu-nets bending actuators [3] and fiber-reinforced actuators [4]. With regard to the configuration, we refer to the humanoid morphology of the soft fingers in [1]. As shown in Figure 3(a), the main body of the HBSF consists of silicone materials, a strain-limiting layer of inextensible but flexible materials (silk screen) in its bottom, and the fiber-reinforcement thread. The strain-limiting layer determines the bending motion of the finger. The fiber reinforcements protect the silicone-based chambers from excessive expansion.

The tubes are used to pressurize the air cavities inside the fingers. A flex sensor (Spectra Symbol FS-L-0095-103-ST) is glued to the flat ventral surface. The structure of the HBSF is like that of a bellows. Referring to the sectional drawing in the transverse plane in Figure 3(b), the most recent version used in the index/middle fingers has 11 segments with a wall thickness of $t = 2$ mm. The two sections of the finger share the same length, so $l_1 = l_2$. The little gap a between segments is equal to 1 mm and is limited by the thin-wall strength of the 3D-printed molds. The distance b between each short bellows is the key parameter that will affect the bending and deflection performance of the

HBSF. An HBSF is divided into four air chambers, which give the fingers four DoF, allowing them to act more like human fingers.

Simulation

Figure 3(c)–(i) presents the simulation results for the soft fingers. The fiber-reinforcement structure is very thin to mesh it into the element based on the FEM. It was therefore omitted in the SOFA simulation. As a result, the input air pressure in the SOFA simulation is less than the one used in a real HBSF, which limits the bending angle of the fingers in the simulation results.

Deflecting the fingers enables several useful collaborative motions between the index and middle fingers. Although the motions in Figure 3(f) and (g) cannot achieve a grip function because of the low stiffness of the soft fingers in the transverse axis, they play a key role in achieving Feix [13] grasp postures 14, 17, 20, 21, and 23 (illustrated later in the article). In addition, the thumb deflection acts in a similar way to the functions shown in Figure 3(h) and (i); the thumb deflects toward or away from the palm for grasping small or larger objects, respectively.

Soft Palm

Function

For human hand grasping, the palm always works collaboratively with the fingers to implement all kinds of manipulations. In this article, the functions of the soft palm are inspired by human palm motion, which includes three main functions: thumb abduction, splaying of four distal fingers, and palmar bending. A key feature of the human hand is thumb abduction and adduction. This allows the thumb to rotate and adjust position and orientation with respect to the manipulated object, which is essential for grasping.

The splaying of the four fingers enlarges the size range of graspable objects. Increasing the angle between the adjacent fingers means that the contact force from the four distal fingers can be evenly distributed to the objects, and it also makes it possible to grip larger objects using two adjacent fingers. Bending the whole plane of the palm is beneficial in facilitating the grasping of smaller objects. Without the help of palm bending, the thumb of the soft hand cannot touch the other fingers, even if all of the fingers are pressurized under the highest pressure and bending at an angle of 180°.

Design

A modular design approach was used for the soft palm. The three functional goals were divided and embedded into two parts: PP-A and PP-B (see Figure 4). The structural design of both parts was inspired by the

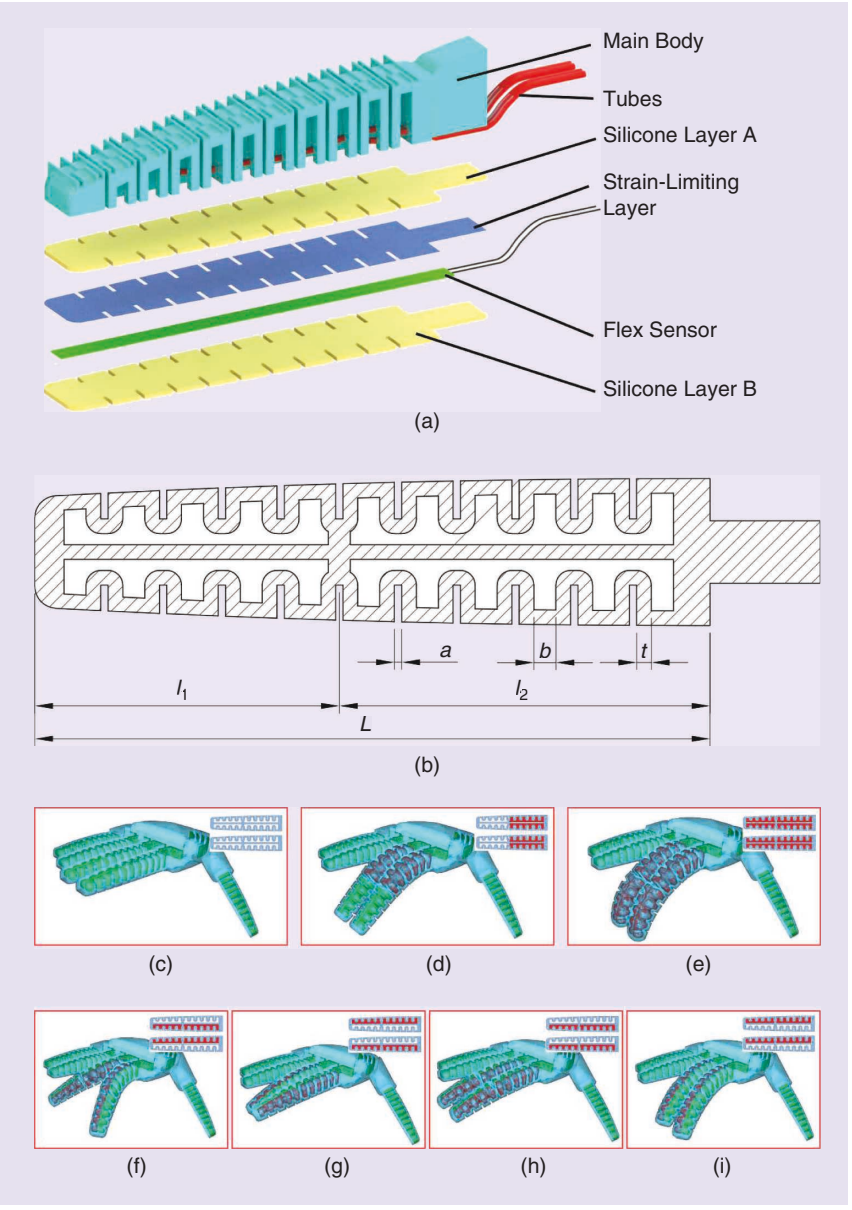

Figure 3. The structure and simulation of the HBSF. (a) A schematic of the components of the HBSF. The fiber-reinforcement structure is depicted by the thin raised features on the main body surface. (b) A sectional drawing (bottom view). The red chambers in (c)–(i) present the pressurized actuators in SOFA [14]. (c) The original morphology. (d) The second section of the index and middle fingers, pressurized. (e) Two sections pressurized together. (f) Deflection of two fingers to enlarge the grasping region. (g) Deflection of two fingers to decrease the gap between them. (h) and (i) Deflection of two fingers to achieve left-right wiggling.

mechanisms of pneu-nets actuators, consisting of network-like chambers inside a silicone body over a strain-limiting layer.

PP-A achieves splaying of the four distal fingers, while PP-B performs the abduction of the thumb and overall bending of the palm. Instead of bending in the manner of pneu-nets actuators, PP-A splays the distal fingers in the palmar plane with a small hump after being pressurized. The main body has four air chambers for actuation [Figure 4(a)]. The four large grooves in front are used to affix the four fingers. The proximal cavity is designed to arrange the pneumatic tubes and sensor wires inside the hands. For PP-B, the bending motion of the palm is achieved by enlarging the horizontal width of the pneu-nets actuator. The widths of the air chambers along the palm were designed to be as wide as possible to generate enough force to bend the palm along with the distal fingers. The tubing tunnel connecting with the bottom cavity in PP-A is used to run the tubes and lines through the palm.

The soft palm uses the same key geometric parameters as the soft fingers, such as wall thickness t and the small gap between segments a. The stiffness of the palm for enabling a reliable support for the other fingers is considered and simulated in the SOFA framework. In addition, a humanoid esthetic design was implemented as a last step, after ensuring that the soft actuators worked as intended and would not affect the performance of the pneumatic actuators.

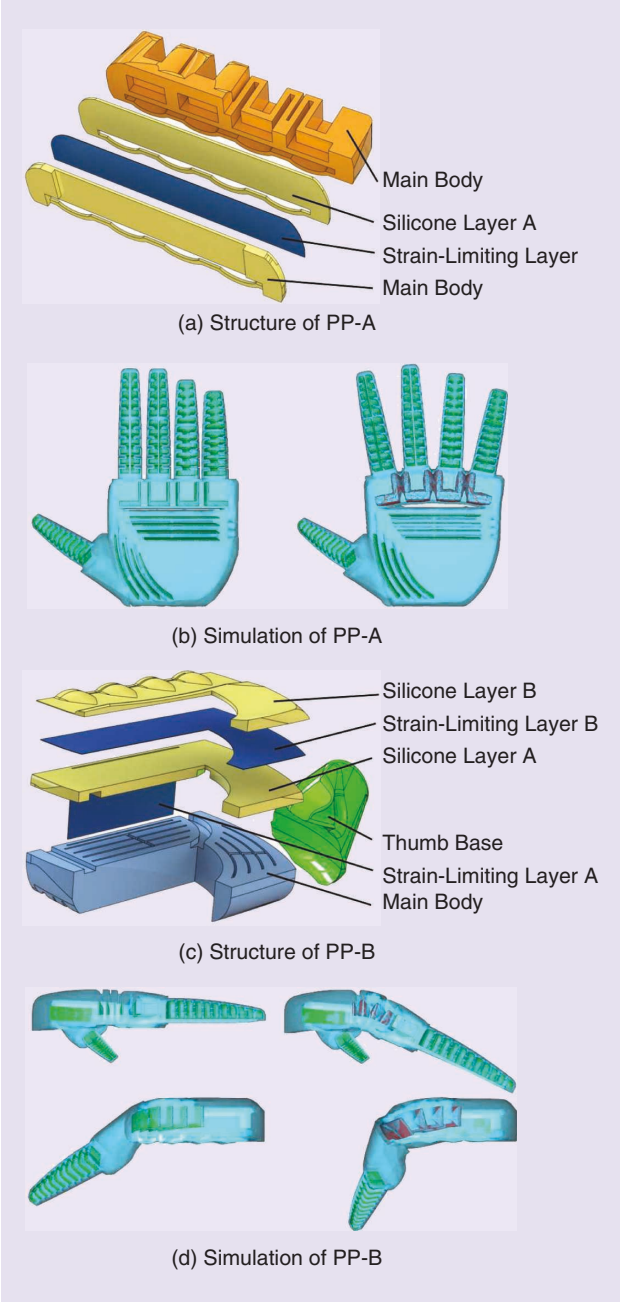

Figure 4. The (a) simulation and (b) structure of the soft palm. (b) and (d) present a comparison of the palm actuators under inflation and deflation states. The red chambers in (b) and (d) represent the pressurized actuators in SOFA.

Simulation

Figure 4(b) and (d) represents the simulation results of the two parts of the soft palm. The three functions of the palm can be clearly detected through the comparison of each actuator before and after pressurization.

Fabrication

Actuator Body Molding

The soft body was fabricated using Smooth-On silicone rubber (Dragon Skin 10 Medium) and Sil-Poxy to obtain a Shore-A hardness of 10. The A and B parts of the Dragon Skin 10 were mixed equally by weight in a plastic cup and then put into a vacuum chamber. Using a vacuum pump, the air trapped in mixed silicone materials expands to bubble and finally collapses under about 0.9 bar vacuum pressure. After evacuation, the silicone material was poured into the molds, as described in Steps 1 and 2 of making the finger, PP-A, and PP-B in Figure 5. The molds were generally left in an upright position to cure for 5 h at room temperature.

Strain-Limiting Layer Sealing

The strain-limiting layer is made of silkscreen fabric and used to ensure that the actuators bend in the desired direction during pneumatic pressurization [3]. The layer was placed in the bottom mold, as in Step 2 of making the finger in Figure 5, and glued together with the bottom sealing portions of all three components. Subsequently, the fabrication of the main body of the actuators was finished, and the chambers inside the silicone body were all sealed. Note that Step 3 of making PP-B does not require molds. The silkscreen fabric was added manually in the reserved gap [Figure 5(h1) and (h2)]. Then, after pouring silicone into the gap and curing, the silkscreen fabric was combined with the main body.

Assembly

Figure 5(j1)–(j4) demonstrates the main procedure of the hand assembly. There are five soft fingers and two soft palm parts in this hand. The same silicone materials were used to bond the different components together by manually pouring liquid silicone on their connecting surfaces. As shown in Figure 5(j1), the proximal ends of the distal fingers are fixed in the large groove mentioned previously. The tubes of each finger are inserted into the bottom cavity inside PP-A.

Figure 5(j2) presents the assembly result of PP-B and a soft–rigid hybrid support. The support consists of silicone skin fitting to the shape of PP-B and the rigid 3D-printed skeleton inside. All the pneumatic tubes go through the support and run out of the hand together. The yellow 3D-printed skeleton of the support is used as the base to fix the hand to the robot arm. As a result, the three parts in Figure 5(j1)–(j3) are assembled together into a soft humanoid hand, as shown in Figure 5(j4). Additionally, to improve the force of friction of the fingertips when grasping objects, three rubber thimbles with nonsmooth surfaces [shown in orange in Figure 5(j4)] are fixed with glue over the fingertips of the thumb, index, and middle fingers.

Control

To control the proposed soft hand under different operating conditions, a controller platform was constructed. Recently, various pneumatic control systems have been designed for position or force control [18]–[20]. In this work, to enable a quick and simple way to evaluate our design, an open-loop control system was implemented so that we could directly control the pressure. The controller platform was implemented based on the proposed design of the Soft Robotics Toolkit (the Fluidic Control

PWM can be expressed as a technique for getting analog results with digital means.

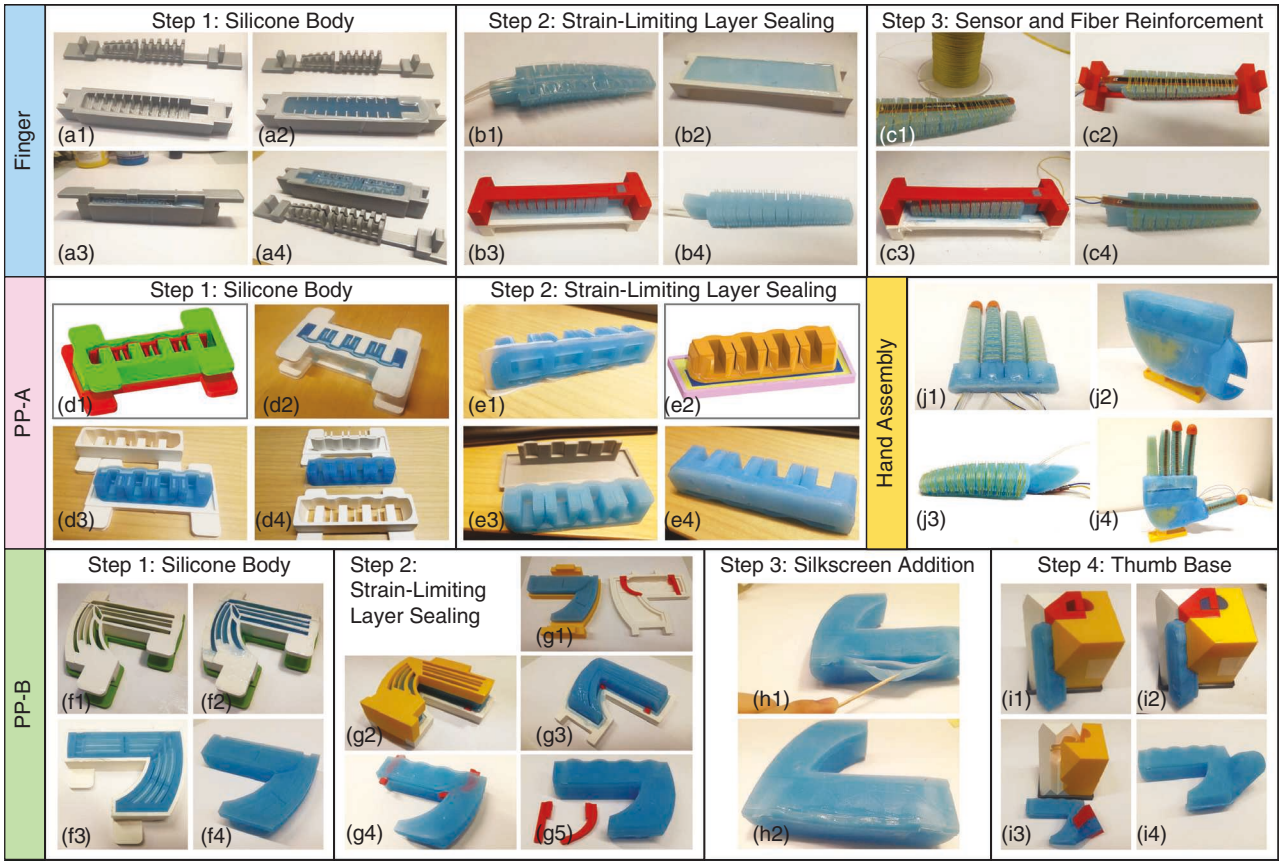

Figure 5. The fabrication process of the soft hand. *Finger*: (a1)–(a4) The main body is made by first pouring silicone material in its bottom mold and then pressing the top mold. (b3) The red part is for clamping and positioning the main body. (c1)–(c4) Fiber and flex sensor fixation to prevent relative displacement when the finger bends. *PP-A*: (d1) The molds. (d2) Pure silicone material. (d3), (d4) The unmolding. In Step 2, the 3D-printed support is used to hold and ensure the thickness of the bottom surface. The process in *PP-B* is similar to the one for *PP-A.* The two red sticks in (g1)–(g5) are used to reserve the space for air tubes and electric wire. The yellow support in (g2) has the same role as the red part in (b3). *Hand assembly*: (j1) The assembly of palm and distal fingers. (j4) The final result.

Board, https://softroboticstoolkit.com/book/control-board). The architecture of our controller board is shown in Figure 6.

The controller board consists of a pneumatic regulator: a set of solenoid valves (SMC-VQ110U-5M Solenoid valve, https://www.smcpneumatics.com/VQ110U-5M.html) to direct the flow of air into the system. The valves are powered and directed by power MOSFET switches. As we want the hand to have as many DoF as possible, we use 20 solenoid valves in total. Thus, each chamber of the finger can be pressurized independently, which allows the hand to have more postures. Two Arduino Mega 2560 Rev3 controllers are used to enable users to interface with the hardware via a serial port connection. The board can be controlled manually (by adjusting switches and potentiometers) or automated via programmed software.

The system pressure is regulated with pulsewidth modulation (PWM), which controls the opening and closing times of the valves at a 60-Hz rate through the Arduino boards. PWM can be expressed as a technique for getting analog results with digital means. One of the most important terms in PWM is the duty cycle. The duty cycle is the proportion of "on" time compared to the total interval, or "period," of time. The duty cycle is expressed as a percentage, with 100% being continuously on and 0% being continuously off. By modulating the value of the duty cycle, analog values can be achieved. Thus, the fixed, regulated input pressure is set to the desired value based on the duty cycle of the PWM signal. With this technique, the finger can easily be controlled to a certain bending angle.

Experiments

Analysis of the HBSF

The HBSFs in this article exhibit novel motion. They deflect in the side-to-side axis, while the bending motion in the grasping axis is still the main function of the soft fingers. After being pressurized, the adjacent inflated segments will generate a mutual force, which achieves the deflection motion. In addition, the number of segments depends on the distance b, as shown in Figure 3(b). When the finger length is defined, a larger b leads to a smaller segment number. When the finger has only one segment, it changes back to the original paradigm of the PneuFlex actuator with two chambers. As shown in Figure 7, to analyze the influence of the segment number on the deflection, six soft fingers with 1, 3, 5, 7, 9, and 11 segments [see Figure 7(c)] were fabricated and tested.

The four air chambers of the HBSF in Figure 3(b) are simplified into two air chambers in Figure 7. The top and bottom sections are intended to imitate the multijoint motion of human fingers. The bending angle [Figure 7(d)] and deflection displacement [Figure 7(e)] were manually measured by CAD software. Some feature points on the fingertip and fixed base were measured to get the bending angle and deflection displacement. Figure 7(k) shows the setup for measuring the grasping force generated by each finger. We gently placed an unpressurized soft finger on top of an electronic pan balance, where the bottom surface of the finger lightly touched the pan. We then tared the weight to reset the scale reading. The top surface of the finger was constrained by the metal plate, which enabled all of the grasping force to be

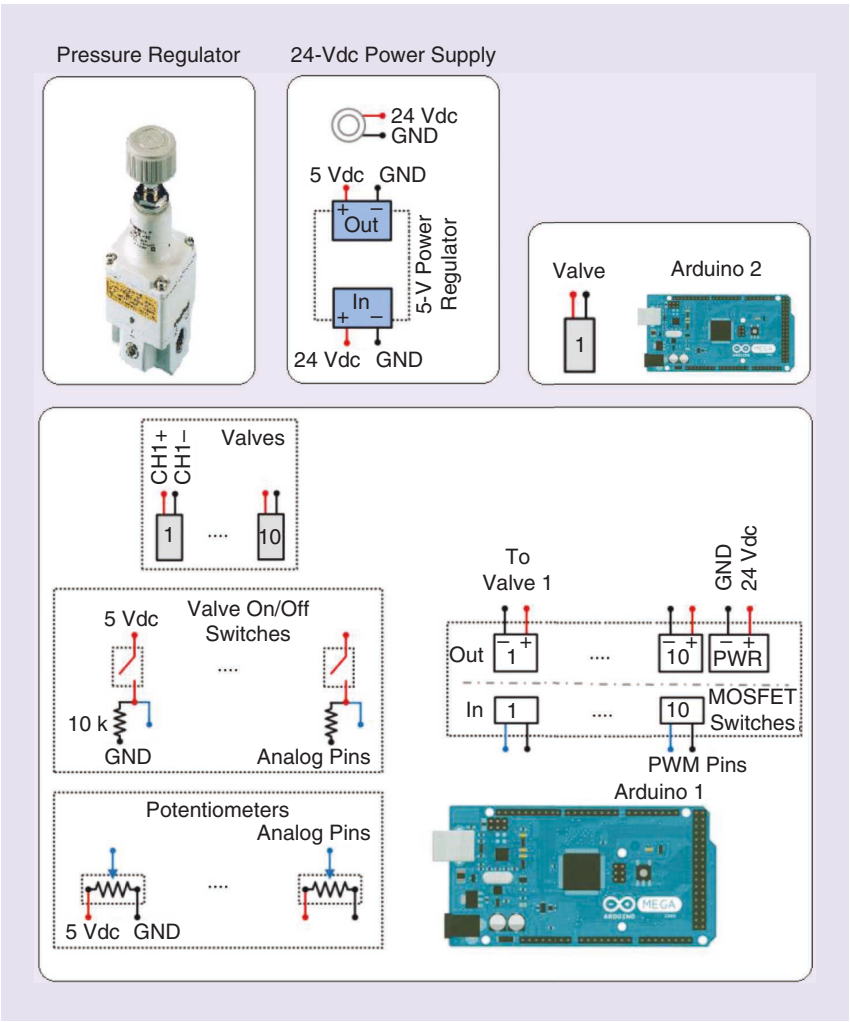

Figure 6. The architecture of the implemented controller board. For clarity, we show only the connection scheme of the Arduino 1 board. The connection scheme of the Arduino 2 is identical to that of Arduino 1. GND: ground; CH: channel.

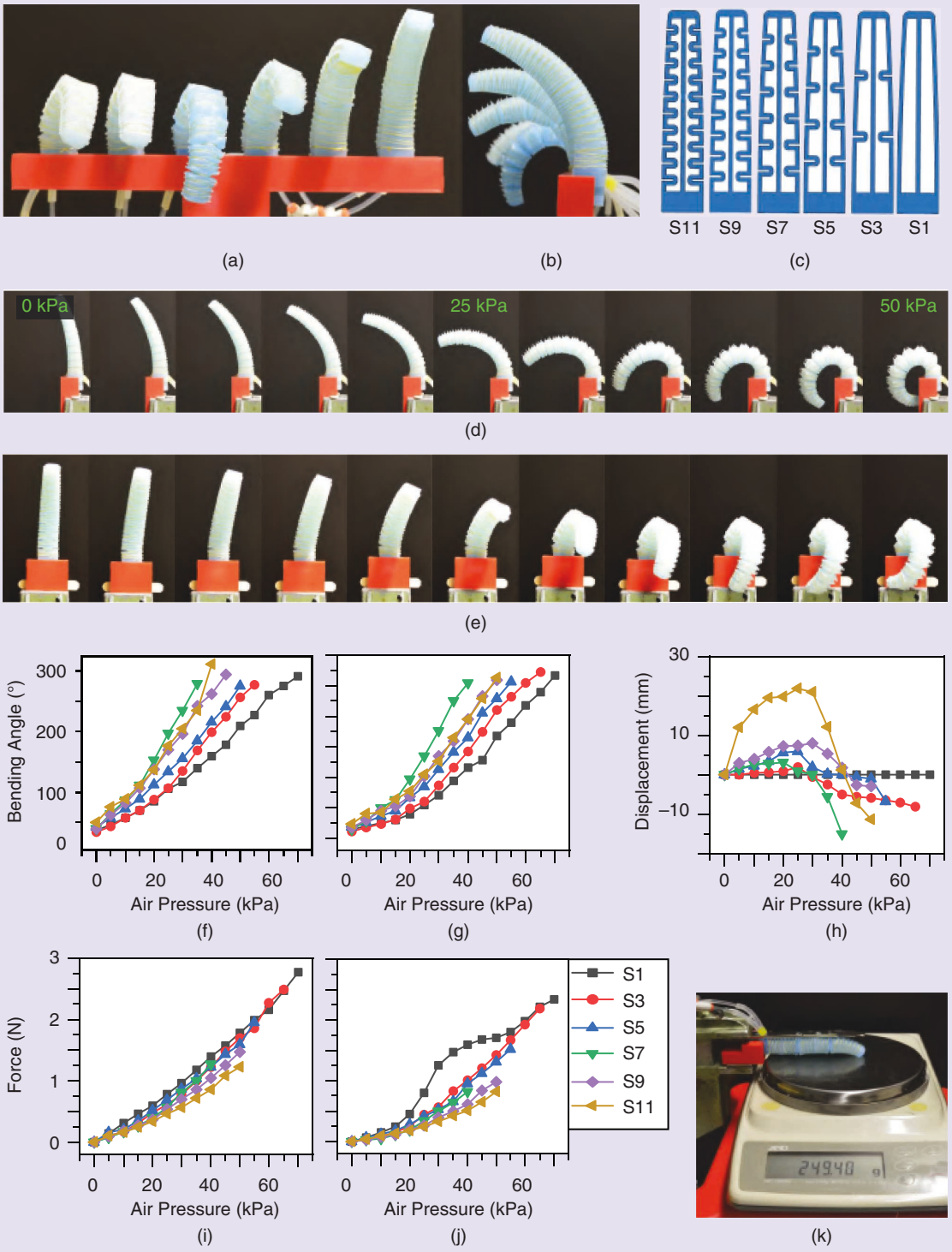

Figure 7. The effect of the number of segments on the bending and deflection motions of six fingers. A comparison of the deflection extent from (a) left to right and from (b) back to front, both through S11, S9, S7, S5, S3, and S1. (c) A sectional drawing of the six fingers. The (d) side and (e) front views of the bending and deflection motions of finger S11 while applying air pressure to a single chamber with 0–50 kPa. The variation of the (f) bending angle and (i) force generated by a finger while applying air pressure equally to both chambers. The variation of the (g) bending angle, (j) finger force generated, and (h) displacement of the fingertip while applying air pressure to a single chamber. (k) The experimental setup for measuring the force generated by a finger.

transmitted to, and measured by, the scale. The weight was estimated via $F = mg$; e.g., the generated grasping force by applying 65-kPa air pressure equally to both chambers of S11 is $249.40 \times 10^{-3} \times 9.8 = 2.44$ N.

According to the test results, the bending angle increases nonlinearly with the applied air pressure, with a relatively slow increase in the low-pressure region and a rapid increase beyond 20 kPa. It is obvious that the variation between the force and bending angle has a close positive correlation. However, it is also noted that, under the same air pressure, fingers with more segments generate larger bending angles and forces when pressurizing both left and right chambers, but they generate smaller angles and forces when pressurizing only a single chamber. This phenomenon actually reflects the different mechanisms of the bending and deflection motions. The greater number of segments means more grooves, which mutually swell during inflation, working as pneu-nets actuators and fewer small sections, which extend during inflation, working as fiber-reinforcement actuators. In addition, as shown in Figure 7(j), the generated grasping force of an S1 finger becomes larger than for those with multiple segments when the applied air pressure goes from 20 to 50 kPa.

Figure 7(h) shows the deflection displacement in the side-to-side axis. The S11 finger has significantly better performance for deflections up to 20 mm [see Figure 7(e) under "25 kPa"]. Combining the experimental results of bending angle and force, the S11 finger is the second most easily driven under double-chamber actuation, and it presents the minimum bending angle under single-chamber actuation. Both characteristics are conducive to enhancing the deflection region of the HBSFs. It is also notable that the finger first wiggles outward in the initial stage of the actuation with lower air pressure and then turns back and wiggles inwards when the bending angle of the HBSFs becomes large at higher air pressure. This results in a loss of efficacy of the deflection motion, even to the point of achieving exactly the opposite displacement. To get the maximum deflection displacement in the side-to-side axis, we selected the key structure parameters of the HBSFs of finger S11 in our new hand. The grasping force of S11 is about 1.23 N and 0.82 N under 50-kPa air pressure applied to both chambers and one single chamber, respectively.

Analysis of the Palm

Figure 8 presents the experimental results for the soft palm. In contrast to the more typical fixed palm, almost all of the parts of our soft palm are deformable, which greatly increases the diversity of hand postures. The measuring method for the palm is the same as that for the HBSF.

Figure 8(e) shows the relationship between the deformation performance and the air pressure of PP-A. It indicates that the splaying angle and force increase slowly when the applied air pressure increases from 10 to 60 kPa and then achieve a rapid increase beyond 60 kPa. Figure 8(a) shows the posture of the hand under 90-kPa air pressure with a splaying angle of 50°. The air pressure should not be more than 100 kPa to avoid collapse.

The influence of gravity on palm bending can be observed in Figure 8(b) and (c). The bending angles of the pronated palm are obviously larger than those of the supinated palm. The maximum angle of the palm-bending motion is 68°, and that of the thumb abduction is about 90°. These two bending ranges can meet most common grasping needs. Without the fiber reinforcement, the two actuators of PP-B should be driven under a safe range of air pressure: lower than 40 kPa.

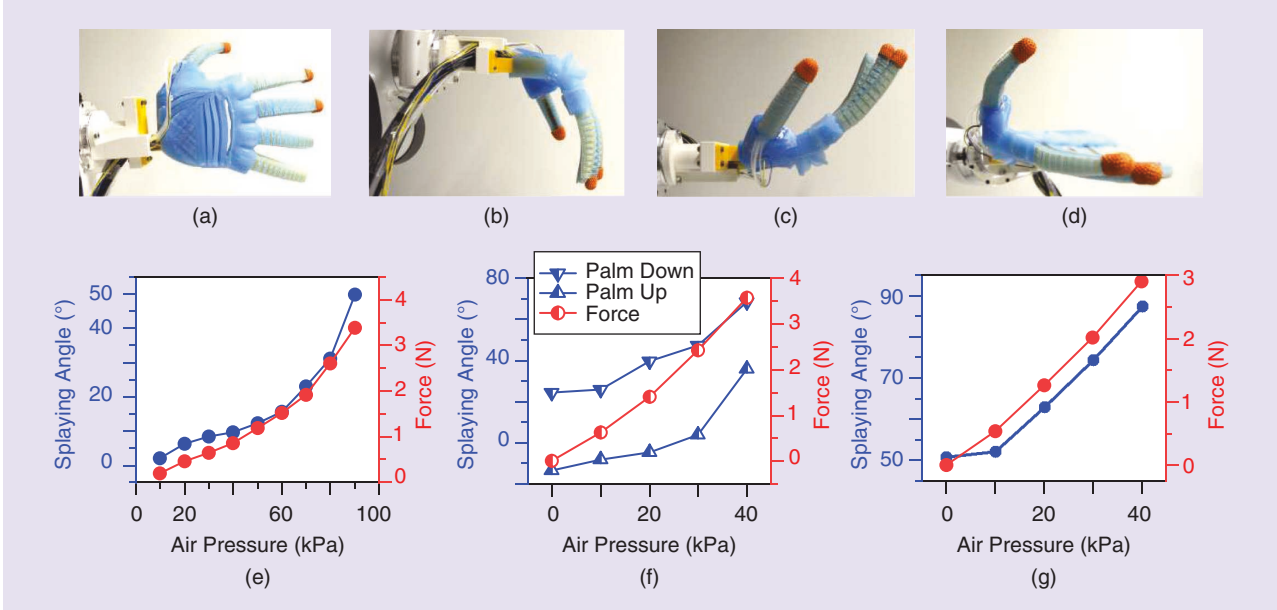

Figure 8. The validation of palm performance on bending angle and output force for (a) and (e) palm splaying; (b), (c), and (f) palm bending with palm down and palm up; and (d) and (g) thumb abduction. The red plots correspond to the red axes.

However, when the object is grasped and in contact with the hand, the pressure can be manually increased to enhance the reliability of the grasp.

Grasping in the Real World

The deflection of the HBSFs can collaboratively work when used as a two-finger gripper to grasp and lift objects that allow the insertion of fingers into the neck portion, as shown in Figure 9(a)–(e). In Figure 9(b) and (c), the index and middle HBSFs illustrate the deflection motion. The gap between the index and middle fingers enlarges noticeably. The bending motion can be used to provide a support force against gravity in the case of the watering can. Furthermore, our hand is able to firmly grasp and lift a relatively large and heavy chair, as seen in Figure 9(f). By applying 50 kPa of pressure, which is a very safe and stable level, to all five soft fingers, the overall grasping force is about $5 \times 1.23 = 6.15$ N. The grasping force of the hand is increased by increasing the air pressure; however, exceeding 70 kPa is not recommended. Figure 9(g) and (h) demonstrates the safety and compliance of the soft hand in human–robot interaction scenarios.

Grasp Dexterity in Feix Taxonomy

To test the grasping performance of our hand, we implemented grasping experiments according to the Feix taxonomy [13], which includes 33 comprehensive grasp types. For every case, the pressures were manually adjusted to reach the desired posture, and the actuation sequences generally followed the principle of actuating the palm first and then driving the fingers. The actuation of the soft palm includes splaying the planar four distal fingers, bending the palm, and abducting the thumb. It helped to first fit the shape and size of the target objects and move the fingers into an appropriate position and orientation. The fingers could then be pressurized to perform the grasping tasks. For splaying, 90 kPa was usually directly applied to PP-A to achieve a relatively large splaying angle. The bending angle and output force were powered by around 30 kPa for PP-B, which sufficed for most scenarios in the practical experiments.

Figure 10 shows photos of 33 grasping posture types from the Feix taxonomy [13]. The success criterion was the hand achieving a position in the Feix taxonomy with stable grasping. Furthermore, the dynamic grasping quality was judged according to up and down movement and rotation of the hand by a Franka Emika Panda robotic arm at a speed of 40 mm/s. This procedure was repeated several times to evaluate the repeatability of the grasps. Our hand failed to perform one stationary grasping posture out of the 33 grasps. The ventral posture failed because the object (the marker pen shown in grasp 32) was thin and long, so the hand could not grasp it firmly. As the bending profile of the soft fingers had a circular shape, the inner diameter of the bending fingers was larger than the diameter of the marker pen, even when reaching a maximum bending angle. From the attached experiment video (available at https://doi.org/10.1109/MRA.2021.3065870) for the 32 successful stationary grasps, the hand successfully passed 31 grasps in the dynamic grasping test. The red ball in grasp 14 dropped in the final stage of moving and rotating. The second photo

It indicates that the splaying angle and force increase slowly when the applied air pressure increases from 10 to 60 kPa and then achieve a rapid increase beyond 60 kPa.

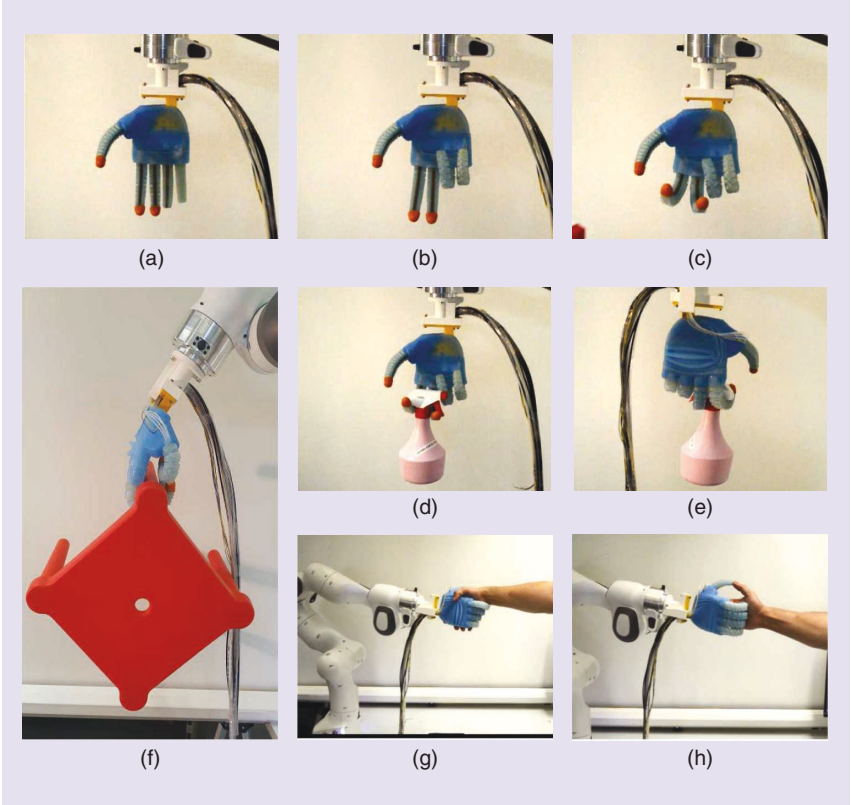

Figure 9. (a)–(e) The ability of our soft-hand prototype to lift a watering can (143 g) by using two adjacent HBSFs. (f) The hand grasping and lifting a chair (541 g). (g) and (h) The safe interaction of the hand with a human.

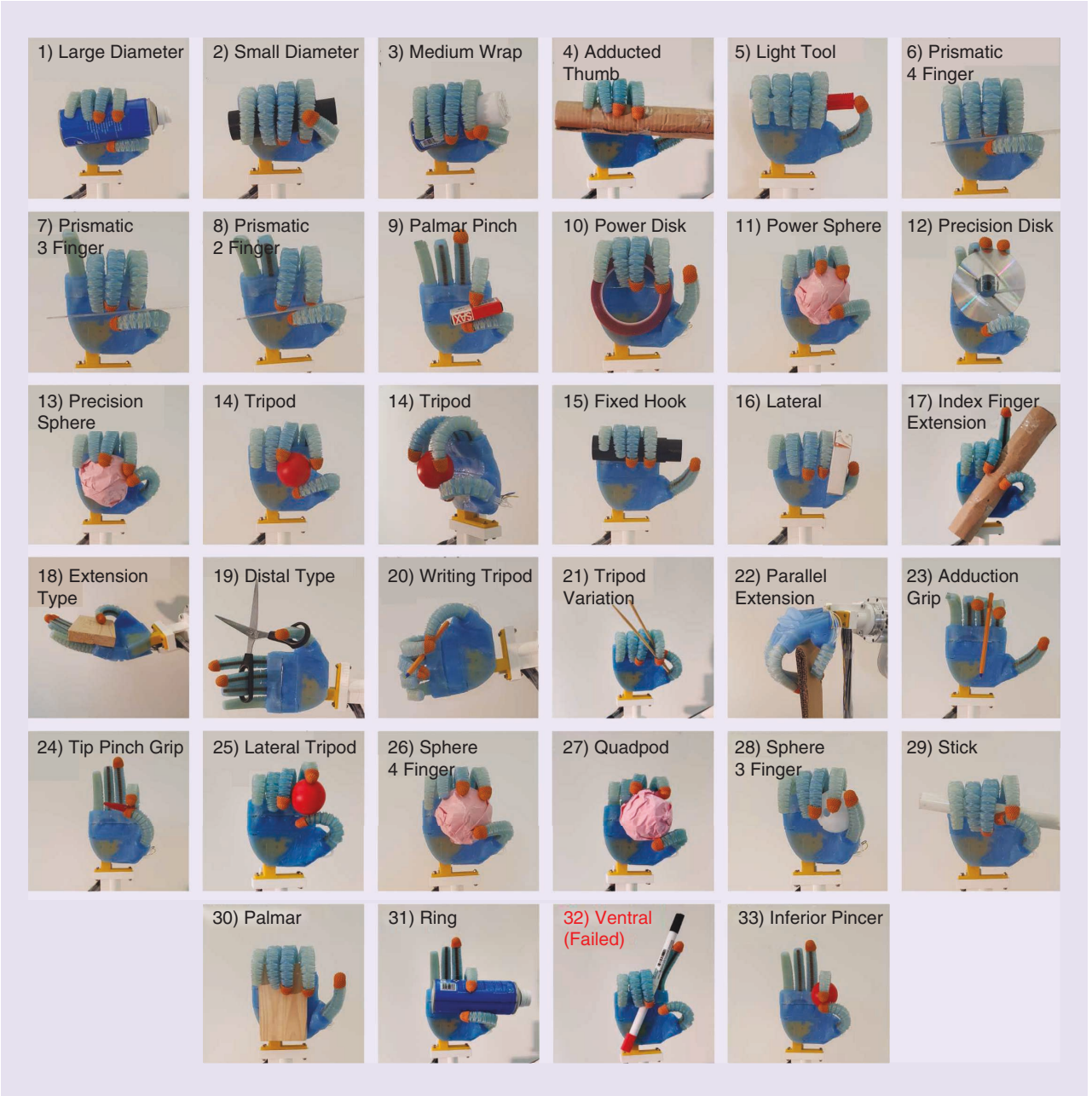

Figure 10. Enacted grasps, numbered according to the Feix taxonomy [13]. Please see the accompanying video for the 32 successful grasps (available at https://doi.org/10.1109/MRA.2021.3065870).

relating to grasp 14 in Figure 10 represents the three-quarter view of the grasping posture. The red ball was fixed by the three fingers without the support of the palm. Because of the inherent compliance of the soft fingers, the red ball was not firmly grasped by the three fingers, and it was finally dropped during the rotation of the hand.

Conclusions

In this article, we have described the development of a new soft humanoid hand capable of grasping different kinds of objects robustly. The hand is compliant, lightweight, and low cost. Its pneumatic actuation enables the soft hand to have high compliance while grasping, allowing it to avoid damaging grasped objects. At the same time, we proposed a new design for a soft finger, the HBSF, and a novel two-part soft palm. The functions of all soft actuators were simulated based on FEM in the SOFA simulator. The experimental results on a series of fingers with different numbers of HBSF segments showed that an HBSF with 11 segments is the best choice for achieving both the bending and deflection motions.

The main advantage of this study is that the postures of the hand can be adjusted with the help of the soft palm, and we can then use different configurations to realize

stable and dexterous grasping. The hand allows us to achieve 32 out of 33 grasp postures in the Feix taxonomy, which demonstrates the postural dexterity of our soft hand. Moreover, 31 of the 32 reachable grasps were shown to be stable.

The design has the limitation that the thumb abduction and the finger splaying angles are limited by the silicone tensile strength and wall thickness of the air-chamber structure. Optimization of the soft palm design so that the thumb can touch the little finger remains for future work. Moreover, integrating sensing in the design would allow improved control to increase safety even further.

Acknowledgments

The first author thanks the China Scholarship Council for financial support through 201906680045 and the Natural Science Foundation of China under grant 51875113. This work is partially supported by CHIST-ERA project Interactive Perception-Action-Learning for Modelling Objects (Academy of Finland decision 326304). This article has supplementary downloadable material available at https://doi.org/10.1109/MRA.2021.3065870, provided by the authors.

References

[1] R. Deimel and O. Brock, "A novel type of compliant and underactuated robotic hand for dexterous grasping," *Int. J. Robot. Res.*, vol. 35, nos. 1–3, pp. 161–185, 2016. doi: 10.1177/0278364915592961.

[2] J. Falco, K. Van Wyk, S. Liu, and S. Carpin, "Grasping the performance: Facilitating replicable performance measures via benchmarking and standardized methodologies," *IEEE Robot. Autom. Mag.*, vol. 22, no. 4, pp. 125–136, 2015. doi: 10.1109/MRA.2015.2460891.

[3] B. Mosadegh et al., "Pneumatic networks for soft robotics that actuate rapidly," *Adv. Funct. Mater.*, vol. 24, no. 15, pp. 2163–2170, 2014. doi: 10.1002/adfm.201303288.

[4] K. C. Galloway, P. Polygerinos, C. J. Walsh, and R. J. Wood, "Mechanically programmable bend radius for fiber-reinforced soft actuators," in *Proc. IEEE Int. Conf. Adv. Robot.*, 2013, pp. 1–6.

[5] A. Lotfiani, H. Zhao, Z. Shao, and X. Yi, "Torsional stiffness improvement of a soft pneumatic finger using embedded skeleton," *J. Mech. Robot.*, vol. 12, no. 1, pp. 1–23, Oct. 2019. doi: 10.1115/1.4045227.

[6] S. Abondance, C. B. Teeple, and R. J. Wood, "A dexterous soft robotic hand for delicate in-hand manipulation," *IEEE Robot. Autom. Lett.*, vol. 5, no. 4, pp. 5502–5509, 2020. doi: 10.1109/LRA.2020.3007411.

[7] Y. Sun, Q. Zhang, and X. Chen, "Design and analysis of a flexible robotic hand with soft fingers and a changeable palm," *Adv. Robot.*, vol. 34, no. 16, pp. 1041–1054, 2020. doi: 10.1080/01691864.2020.1777197.

[8] C. B. Teeple, T. N. Koutros, M. A. Graule, and R. J. Wood, "Multi-segment soft robotic fingers enable robust precision grasping," *Int. J. Robot. Res.*, vol. 39, no. 14, pp. 1647–1667, 2020. doi: 10.1177/0278364920910465.

[9] P. Polygerinos et al., "Modeling of soft fiber-reinforced bending actuators," *IEEE Trans. Robot.*, vol. 31, no. 3, pp. 778–789, 2015. doi: 10.1109/TRO.2015.2428504.

[10] J. Fras and K. Althoefer, "Soft biomimetic prosthetic hand: Design, manufacturing and preliminary examination," in *Proc. IEEE/RSJ Int. Conf. Intell. Robots Syst.*, 2018, pp. 6998–7003.

[11] K. C. Galloway et al., "Soft robotic grippers for biological sampling on deep reefs," *Soft Robot.*, vol. 3, no. 1, pp. 23–33, 2016. doi: 10.1089/soro.2015.0019.

[12] W. Hu and G. Alici, "Bioinspired three-dimensional-printed helical soft pneumatic actuators and their characterization," *Soft Robot.*, vol. 7, no. 3, pp. 267–282, 2020. doi: 10.1089/soro.2019.0015.

[13] T. Feix, J. Romero, H. Schmiedmayer, A. M. Dollar, and D. Kragic, "The grasp taxonomy of human grasp types," *IEEE Trans. Human-Mach. Syst.*, vol. 46, no. 1, pp. 66–77, 2016. doi: 10.1109/THMS.2015.2470657.

[14] J. Allard et al., "SOFA—An open source framework for medical simulation," in *Medicine Meets Virtual Reality*, Palm Beach, FL: IOP Press, pp. 13–18, Feb. 2007, v19.12.00.

[15] C. Duriez, "Control of elastic soft robots based on real-time finite element method," in *Proc. IEEE Int. Conf. on Robotics and Automation (ICRA)*, 2013, pp. 3982–3987.

[16] E. Coevoet et al., "Software toolkit for modeling, simulation, and control of soft robots," *Adv. Robot.*, vol. 31, no. 22, pp. 1208–1224, 2017. doi: 10.1080/01691864.2017.1395362.

[17] M. Pozzi et al., "Efficient fem-based simulation of soft robots modeled as kinematic chains," in *Proc. IEEE Int. Conf. on Robotics and Automation (ICRA)*, 2018, pp. 4206–4213.

[18] R. Deimel, M. Radke, and O. Brock, "Mass control of pneumatic soft continuum actuators with commodity components," in *Proc. IEEE/RSJ Int. Conf. on Intelligent Robots and Systems (IROS),* 2016, pp. 774–779.

[19] A. D. Marchese and D. Rus, "Design, kinematics, and control of a soft spatial fluidic elastomer manipulator," *Int. J. Robot. Res.*, vol. 35, no. 7, pp. 840–869, 2016. doi: 10.1177/0278364915587925.

[20] D. P. Holland et al., "The soft robotics toolkit: Strategies for overcoming obstacles to the wide dissemination of soft-robotic hardware," *IEEE Robot. Autom. Mag.*, vol. 24, no. 1, pp. 57–64, 2017. doi: 10.1109/MRA.2016.2639067.

Haihang Wang, College of Mechanical and Electrical Engineering, Harbin Engineering University, Harbin, 150001, China. Email: wanghaihang@hrbeu.edu.cn.

Fares J. Abu-Dakka, Intelligent Robotics Group, Department of Electrical Engineering and Automation, Aalto University, Espoo, 02150, Finland. Email: fares.abu-dakka@aalto.fi.

Tran Nguyen Le, Intelligent Robotics Group, Department of Electrical Engineering and Automation, Aalto University, Espoo, 02150, Finland. Email: tran.nguyenle@aalto.fi.

Ville Kyrki, Intelligent Robotics Group, Department of Electrical Engineering and Automation, Aalto University, Espoo, 02150, Finland. Email: ville.kyrki@aalto.fi.

He Xu, College of Mechanical and Electrical Engineering, Harbin Engineering University, Harbin, 150001, China. Email: railway_dragon@sohu.com.